

# The equine nuchal ligament 1: structural and material properties

K. S. Gellman, J. E. A. Bertram<sup>1</sup>

Department of Biomedical Sciences, College of Veterinary Medicine, Cornell University, Ithaca, New York, USA,

<sup>1</sup>Department of Nutrition, Food & Exercise Science, Florida State University, Tallahassee, Florida, USA

## Summary

The nuchal ligament, a large elastic structure in the dorsal cervical region, helps support the head and neck in the horse. During locomotion, the caudal funicular and cranial lamellar regions make the largest contribution to elastic strain energy storage. By storing and returning strain energy, the nuchal ligament reduces the amount of oscillatory head movements. These conclusions are derived from examination of the functional morphology of the equine nuchal ligament, its deformation during head movements, and the measurements of the mechanical properties of the tissue using a loading frame. The modulus of elasticity (Young's Modulus) was found to be similar to published values for bovine nuchal ligament:  $8.4 \times 10^5$  ( $0.2 \times 10^5$  S. E.). The measured material properties can be combined with an analysis of tissue strain, and structural organization, to provide detailed estimates of the passive contribution of the nuchal ligament to locomotory motions of the head and neck.

## Keywords

Equine, Nuchal Ligament, Biomechanics, Elastin, Young's Modulus

Vet Comp Orthop Traumatol 2002; 15: 1–6

## Introduction

The vertebrate nuchal ligament (NL) is an elastic structure on the dorsal midline between the occiput, the cervical vertebrae and the cranial thoracic spinous processes. It is highly developed in many artiodactyls, but can be rudimentary or absent in birds, carnivores and primates. The classical interpretation of NL function is: that it supports the head in an alert position, yet stretches to accommodate the lowered head in the grazing position (3, 4). However, these studies suggest that the equine NL is almost unstrained when the animal holds its combined head and neck segment in an alert position, and so the NL can offer little static support under these circumstances. At the other extreme, if the grazing position were achieved simply by stretching the nuchal ligament, the NL would probably be stretched beyond its range of elastic compliance. Despite these contradictions, the NL exists as a large and elegantly organized structure of the neck. The role of the NL during locomotion has only recently been investigated (6). It may be that traditional anatomists have overestimated the structural support role and underestimated the locomotory importance of the NL.

The NL of the ungulates has a very high proportion of the highly extensible biological polymer elastin. At 80% elastin content by dry weight (8, 10), the NL has a characteristic yellow colour and shows long-range reversible extensibility. However, the properties of the NL, as a tissue, are different from those of purified elastin. Electron microscopy and freeze-etch studies of bovine NL have revealed that the elastic

fibres are surrounded with a matrix of interwoven collagen fibrils, lying parallel to the main ligament axis, and intermittently linked to the elastic fibres with thin filaments (9). These authors conclude that the nuchal ligament may be considered a fibre-reinforced composite material composed of stiff fibres (collagen) immersed in an amorphous elastic matrix. The mechanical behaviour of the NL is the result of the combined properties of its components.

On the gross level, the NL is a symmetrical paired structure joined on the dorsal midline. The equine NL consists of a dorsal cord-like section (funicular) joined to a flat, sheet-like section (lamellar) (Fig. 1). It is contiguous with the predominately collagenous supraspinous ligament of the thorax. The elastin content of the cranial supraspinous ligament increases between T8 and T4, where it becomes the composite described above (4). The funicular part is broad and flat at its origin on the cranial thoracic spines, and becomes more cord-like and narrow towards its insertion on the skull. The fibre bundles of the lamellar part are closely interwoven with those of the funicular part, with the lamellar bands coursing cranio-ventrally to insert on the dorsal spines of cervical vertebrae two through six. The most cranial lamellar band, inserting on the axis (C2), is the longest and most robust (Table 1), equivalent in cross-sectional area to the caudal funicular segments. The prevalent mechanical force, acting on the combined head and neck segment, is gravity, which is passively countered by the tensile forces of the NL and actively by the epaxial cervical musculature. Although the ultimate range of motion of the combined head and neck seg-

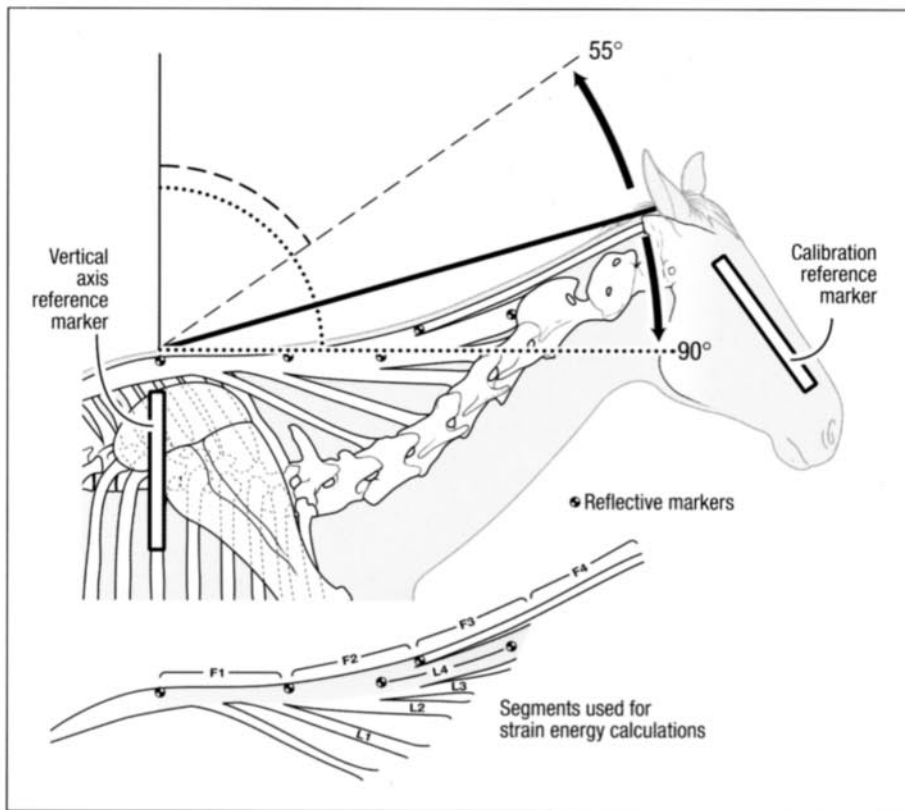


Fig. 1 *Ex vivo* measurement of elastic strain energy in the nuchal ligament. The neck angle was measured between the poll, the withers and the vertical projection of a reference marker perpendicular to the ground. The head was moved from an alert, unstrained position ( $55^\circ$ ) to a horizontal position ( $95^\circ$ ), so that the locomotion range of  $55^\circ$ – $90^\circ$  would be within the limits of the data. The reference marker on the horse's head is used to calibrate the distance for the strain measurements. The inset diagram shows the functional divisions of the nuchal ligament. The regions are labeled from proximal to distal, with F = funicular, and L = lamellar. The shaded regions are those whose structural properties allow substantial strain energy storage.

Subject	Mass (kg)	F-1 ( $\text{cm}^3$ )	F-2 ( $\text{cm}^3$ )	L-4 ( $\text{cm}^3$ )
1	490	320	74	143
2	489	275	68	158
3	483	217	64	188
<b>Mean (S.D.)</b>	<b>487 (4)</b>	<b>271 (52)</b>	<b>69 (5)</b>	<b>163 (23)</b>

Table 1  
Volume of nuchal ligament segments implicated in locomotion

ment is defined by the structural limitations of the cervical vertebrae and their attachments (2), the range of motion observed in normal physiological activities, such as locomotion, is much more limited (6).

The studies undertaken in this paper, and the following paper (6), aim to investi-

gate the structural and functional properties of the equine nuchal ligament through a series of *in vitro*, *ex vivo* and *in vivo* analyses. Measurements of the structural and material properties presented in this paper will be used for the dynamic functional analysis in the second paper.

## Methods

### Subjects

Five healthy adult horses, euthanatized for reasons unrelated to musculo-skeletal problems, were used for portions of the analyses conducted. A nine years old grade gelding, a 13 years old Arab mare, an 18 years old Paint gelding and an 11 years old Thoroughbred gelding were used for morphometric analysis of the head and neck and mass distribution. The first three horses were also used for measurement of *ex vivo* NL deformation. The excised NL, from all four of these animals plus a five year old Standardbred gelding, were tested to determine the NL material properties as described below. The excised specimens were kept moist in physiological saline and refrigerated until use, which was within 24 hours of euthanasia.

### Morphometry

Excised nuchal ligaments, with fat and adventitia removed, were divided into functional regions (see Fig. 1, inset). The divisions were equidistant on the funicular segment, and divided by branch for the lamellar segment. The volume of each was determined by water displacement in a large graduated cylinder.

### Measurement of Nuchal Ligament Strain during Head Movement, *ex vivo*

The aim of this analysis was to measure changes in NL length imposed solely by the position of the combined head and neck segment. Deformation in the length of the NL can then be related to force per unit volume through the force/deformation relationship of the elastic fibres tissue. The animals were euthanatized by captive bolt, and prepared immediately for the experiment. The measurements were completed within 90 minutes of euthanasia. Each subject was placed in lateral recumbancy to eliminate deformation of the NL due to

gravitational forces. The skin and musculature of one side of the neck were removed, exposing the lateral aspect of the NL from T6 to the occiput. Small reflective markers (1 cm in diameter) were sutured to the ligament, dividing it into the functional segments shown in Fig. 1 (inset). The head was held at a neutral angle, relative to the neck (approximately 90°), and affixed to a wooden sledge that held the head and neck in an undistorted sagittal plane. The combined head and neck segments were then moved manually, through the full range of physiological motion (Fig. 1). This experimental range was determined *in vivo* by kinematic analysis (6) and is defined by the angle between the dorsal aspect of the neck and a vertical projection at the withers, perpendicular to the ground surface. In the *ex vivo* subjects, adhesive tape was placed on the scapula of the animal while it was standing, prior to euthanasia, to mark the angle perpendicular to the ground for the visual field. The reflective markers were videotaped from an orthogonal view five meters above the cadaver in order to reduce lens parallax. Subsequently, individual video fields were calibrated, digitized and analyzed using a digital image analysis programme<sup>1</sup>. The change in distance between markers (indicating segment strain), and the angle formed by the head and neck with reference to the vertical projection at the withers, were measured in representative fields throughout the range of motion.

Logarithmic, or true strain was calculated for each NL segment using the equation:

$$\epsilon = \ln [l_t / l_0] \quad (1)$$

where  $\epsilon$  is strain,  $l_0$  is the original measured length of the segment at 55° head angle, and  $l_t$  is the instantaneous length. For each NL segment in each animal, the strains from multiple trials were fitted to a linear regression curve. The predicted values from

each animal were plotted together, and a linear regression was fitted to the group for each NL segment. These regression equations correlate the tissue strain to the angle of the neck. The range of neck angles studied *ex vivo* encompassed those seen in kinematic analysis: from 55° when the head is fully raised, to 95° when the head is fully lowered (6).

### Testing Material Properties

The nuchal ligaments from five cadaver horses were used to characterize the material properties of the equine NL. Sections of fresh ligament from the lamellar and funicular segments were affixed to a material testing frame<sup>a</sup>, using cryo-clamps (refrigerated by circulating liquid N<sub>2</sub>). Samples were pooled to provide a characterization of NL properties because consistent differences between regions were not detected. These results are consistent with previous reports of the NL in artiodactyls. From fixed microscopic sections, the material property consistency throughout the equine NL was also implied by the similarity in histological organization. The specimens taken from these two regions of the NL were easily adapted for use in the test frame clamps, being thin enough to be securely clamped, and having a symmetrical geometry along a sufficient length. The surface of the tissue was cleaned of all adventitia, and reference marks (fiducial) were applied using India ink. The fiducial marks were placed approximately 4 cm apart in the centre of the specimen at least 2.0 cm from the clamp. The strain was measured between these marks, while avoiding any stress concentrations at the tissue/clamp interface. The distances between the marks, measured accurately with calipers for each specimen, were used to normalize the individual specimen's tissue length when processing the force-deformation data. The tissue was kept moist with a spray of physiological saline throughout the testing period. Samples were subjected to controlled tensile oscillations at rates ranging from

2–8 mm/s, 8 mm/s being the maximum velocity of the testing frame. A few were tested to failure. In most cases, failure occurred at the clamp interface, rather than between the fiducial marks, where strain was measured accurately. The samples were not specifically preconditioned, however, and significant differences were not noted between early and late trials of individual samples.

Each sample was subjected to 4–12 trials. At the start of each trial, the frame was retracted so that the tissue was slack and not under any tension. Using a video-dimensional analyzer<sup>b</sup>, changes in the length of each specimen during the trial were measured as the changing distance between the fiducial lines. After each specimen was tested, the cross-sectional area of the tested region was measured by video-digitization of frozen cross-sections. Individual video fields were calibrated from a marker placed in the field, digitized and, using a digital image analysis program, measured. The cross-sectional area, multiplied by the length of the segment, equals the volume of each specimen, which is used to normalize directly measured force to stress (force per unit area) in the ligament.

Logarithmic, or true strain was calculated for each NL segment using equation (1). Although nominal (engineering) strain ( $\epsilon = [l_t - l_0] / l_0$ ) is more commonly used, for a highly deformable biological tissue, true strain is often preferred. True strain uses the instantaneously changing length of the segment rather than the initial length as comparison (10). Similarly, stress was calculated as true stress:

$$\sigma = F / A_t \quad (2)$$

where  $\sigma$  is stress,  $F$  is the force required to deform the tissue, and  $A_t$  is the instantaneous cross-sectional area. Since volume does not change, as the specimen lengthens, the cross-sectional diameter will decrease. For a highly deformable tissue, as load is applied, the instantaneous cross sectional area will describe the NL force distribution

<sup>1</sup> The analysis was performed on a Macintosh computer using the public domain NIH Image v. 1.57, developed at the U.S. National Institutes of Health and available on the internet at <http://rsb.info.nih.gov/nih-image/>

<sup>a</sup> Sintech I/S, MTS, Eden Prairie, MN

<sup>b</sup> Instrumentation for Physiology and Medicine, Inc., San Diego, CA

more accurately than the initial area measured at the resting length. The instantaneous cross-sectional area was calculated by dividing the volume by the length of the segment for each data point. Young's modulus was calculated separately for the compliant (< 50% strain) and the stiff (> 70% strain) portions of the stress/strain curve. For comparison with NL properties of other species, the linear slope of the compliant region (Young's modulus) of the stress/strain curves was found individually for each trial for the range of strain 0–0.50 and averaged for each sample.

To more accurately describe the compliant region, a polynomial equation was fitted to that portion of the curve. For each tissue sample, stress/strain data for all trials were plotted together and fitted to a second order polynomial. The predicted values from the polynomial regressions for each of 18 samples were plotted together, and a "master" curve was fit to the entire data set.

## Statistical Analysis

The material properties sample group was too small to evaluate how well it fitted a Gaussian distribution, and so tests assuming normal distribution could not be used. The moduli of elasticity (Young's Modulus) values from the funicular segments were compared to values from the lamellar segments using a Wilcoxon Rank Sum Test, and the difference between the groups was not significant.

## Results

Apparent differences were not observed as a result of age, sex, nor breed in the nuchal ligaments of these animals. It was noted that, in the extremely upright positions (< 60°), the NL was slack and unstrained. In lateral recumbancy, without any

influencing musculature, the neutral position of the combined head and neck segment (i.e. the neck position imposed by the retraction of the NL) tended to be approximately 55°. At a neck angle of 55 degrees, all portions of the NL are unstrained. The more cranial portions of the funicular, and caudal portions of the lamellar ligament have little tissue volume (15% of the volume of the F1, F2 and L4 segments) and underwent limited strain (8–15% strain compared to 20–35% for the F1, F2 and L4 segments). These portions have been neglected from the remainder of the analysis because it is doubtful that they store a useful quantity of elastic energy. However, it is possible that under certain circumstances, the remainder of the segments combined could increase the strain energy storage of the NL by as much as 20%.

Functional load bearing, in the equine nuchal ligament, passes from its origin on the cranial thoracic spinous processes, through NL regions F-1 and F-2, then to region L-4, inserting on the second cervical vertebrae (Fig. 1). This determination was based upon strain observed in each segment during movement in the physiological range for locomotion and the volume of tissue in each segment: force-transmitting capacity is dependent upon both of these values. It is assumed that the connection to the supraspinous ligament and cranial dorsal spinous processes provide a stable anchor to the main trunk of the animal. Although some of the cranial funicular segments are deformed during head movement, their small tissue volume precludes any sizable strain energy storage capacity. The relationship of neck angle to NL strain was characteristic for each functional region (Fig. 2). The cranial lamellar region showed greater strain than the caudal funicular regions at all neck angles measured.

Forced elongation of the NL shows the classic J-shaped curve of a collagen re-enforced compliant structure (Fig. 3) (10). The sample shown has been strained to almost 90% greater than its original length, but it retains high compliance (low stiffness) until it is 80% greater than its resting length. At that point, there is a focal change in the stiffness of the NL: its modulus of elasticity,

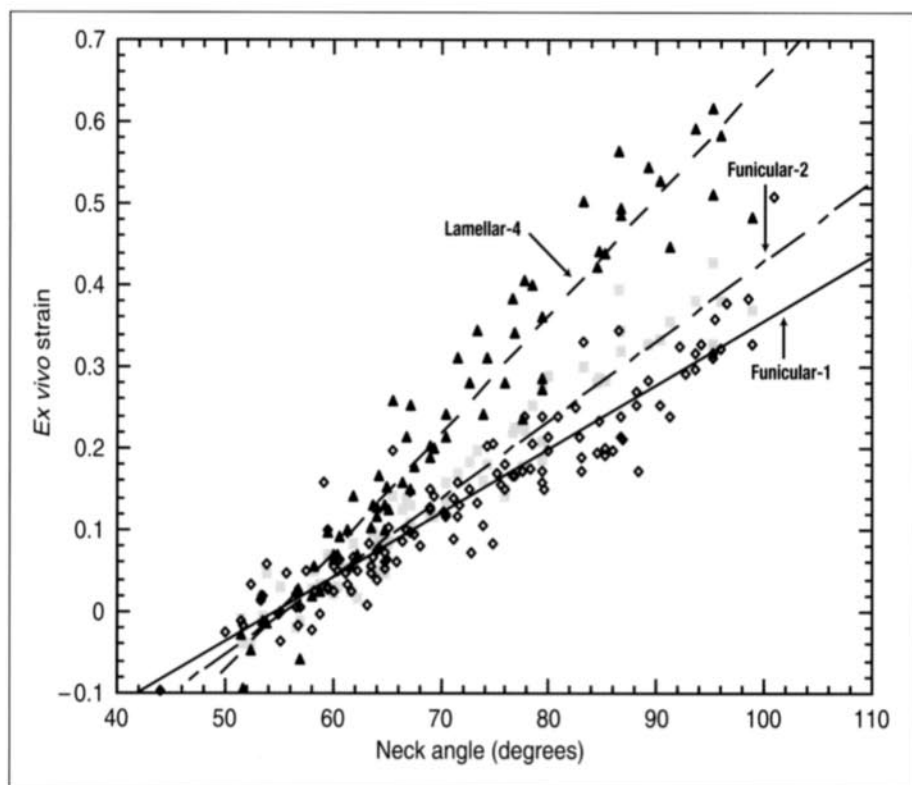


Fig. 2 Ex vivo nuchal ligament strain values. These are plotted for three animals for the three functional regions of interest. The strain was calculated by normalizing deformation of each nuchal ligament region to its length at 55°. Linear regressions are fit to each region as follows:

Funicular 1:  $\epsilon = -0.43 + 0.01d$  ( $R = 0.94$ ); Funicular 2:  $\epsilon = -0.53 + 0.01d$  ( $R = 0.97$ ); Lamellar:  $\epsilon = -0.79 + 0.01d$  ( $R = 0.97$ , where  $\epsilon$  is strain, and  $d$  is degrees of neck angle with respect to the withers).

as characterized by the slope of the plot, increases by more than two orders of magnitude.

The NL strain levels observed in normal locomotion range from 15% to 45%, so only the compliant portion of the curve is relevant to locomotion analysis (6). However, in this region of interest, a linear regression does not closely predict the measured stress. For this reason, a master stress/strain curve (Fig. 4) was plotted from the actual stress/strain data (18 samples from 5 animals). The master curve for the 0-60% strain region was found to be:

$$\sigma = 2.3 \times 10^4 - 1.5 \times 10^5 \epsilon + 2.1 \times 10^6 \epsilon^2 \quad (R = 0.96) \quad (3)$$

The testing device used had a maximum extension velocity of 8 mm/second. From kinematic data, the fastest extension rate for the entire length of the NL (~750 mm) at the canter was found to be ~200 mm/s. Scaled for a 40 mm section, as used in the material testing, the *in vivo* extension rate is approximately 10.67 mm/s, which is close to the 8.0 mm/s test rate.

The mean modulus of elasticity (Young's Modulus) for the entire data set (18 samples, five animals) over the 0-50% strain range was found to be:  $8.4 \times 10^5$  ( $0.2 \times 10^5$  S. E.).

## Discussion

### Strain Energy Storage Capacity of the Nuchal Ligament

The mechanical work capacity of the nuchal ligament *in vivo* is determined by both its material and structural properties. The *ex vivo* manipulations indicate that elastic energy storage potential, which is the product of strain (normalized deformation) and stress (force per cross-sectional area), is maximized in segments F1, F2, and L4 (see shaded inset, Fig. 1), creating a functional support guy between the relatively rigid attachment of the NL at the withers, and the second cervical vertebra. In order to simplify the analysis, only the NL segments capable of substantial strain

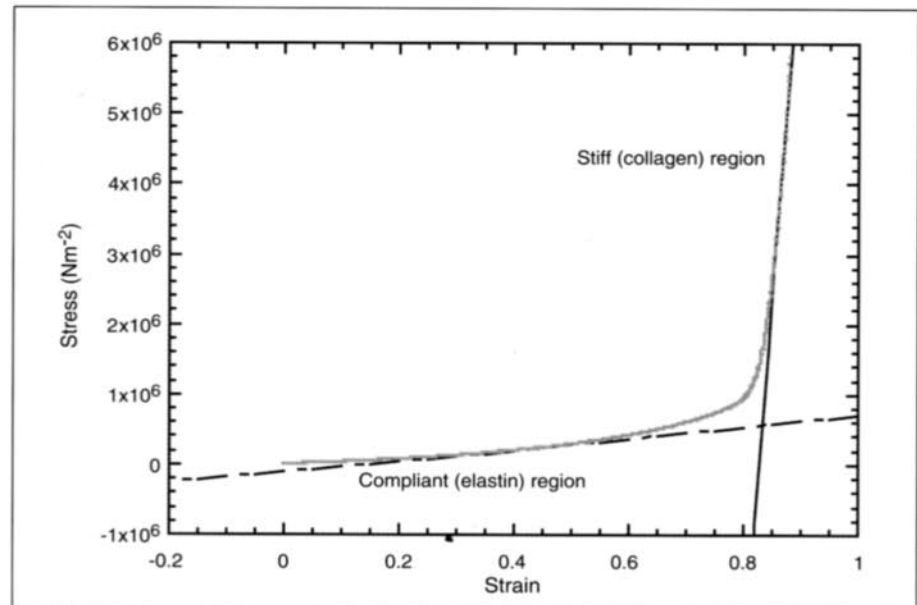


Fig. 3 Stress and strain of an individual sample *in vitro*. An individual stress/strain curve is shown, with regression lines fitted separately to the compliant and stiff portions of the curve. The slope of the regression equation is Young's Modulus, the normalized measure of material stiffness. The equation describing the compliant zone (0-70% strain) is:  $\sigma = -8.3 \times 10^4 + 8.15 \times 10^5 \epsilon \text{ Nm}^{-2}$  ( $R = 0.97$ ). The equation describing the stiff zone (80-85% strain) is:  $\sigma = -8.48 \times 10^7 + 1.03 \times 10^8 \epsilon \text{ Nm}^{-2}$  ( $R = 0.99$ ). Young's modulus for the compliant zone,  $8.16 \times 10^5 \text{ Nm}^{-2}$ , approaches the published values for isolated elastin fibres ( $6 \times 10^5 \text{ Nm}^{-2}$ , Wainwright et al., 1982), and the modulus for the stiff zone,  $1.0 \times 10^8 \text{ Nm}^{-2}$  indicates the properties are dominated by the collagen component.

energy storage during locomotion are presented. While the lamellar segments attached to C3-C6 have substantial volume, they experience little deformation (only

8-12%) during the range of motions seen in normal locomotion, and so do not contribute very much to this activity. It may be that these caudal lamellar segments play an

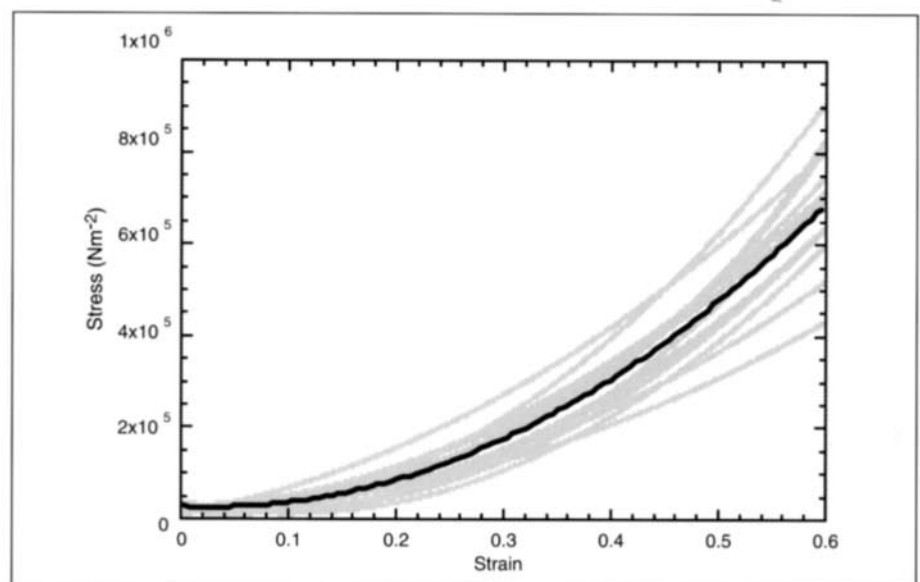


Fig. 4 Master curve of nuchal ligament stress/strain. Polynomial regression curves are plotted for each sample tested ( $n = 18$ ), in the compliant range (0-60% strain). The mean (master) curve is shown by the heavy line. This relationship is used to calculate nuchal ligament stress ( $\text{Nm}^{-2}$ ) from nuchal ligament strain found *in vivo*.

important role in lowering the head to the ground for grazing, but that is outside the scope of this study. Similarly, while the cranial funicular region (rostral to the C3–4 level) was shown in our preliminary experiments to have increases in length up to 20% when the head was flexed independently; the attenuation of the NL in the cranial region leaves a very small amount of tissue for strain energy storage. The capacity for strain energy storage is dependent upon both the magnitude of strain and the structure's cross sectional area.

Although there is some variation in head angle during locomotion, the fixed head angle of 90° was chosen, based upon an average position observed in Standard-bred horses during *in vivo* studies. (6). Although galloping horses may exhibit considerable head extension, at the cantering velocity used in this study (8 m/s) this was not observed. Assuming a fixed head position enabled the *ex vivo* portion of the study to be simplified. Clearly, a given horse's habitual head angle can vary according to training, as well as the speed of running. However, because the head angle primarily affects strain of the cranial funicular NL, it is not an important consideration for this analysis.

These findings do not explain the very important issue of head flexion in collected performance horses, which is intrinsically linked to the simultaneous engagement of the hindquarters and relaxation of the poll. Because the centre of mass of the horse's head is located very near to the atlanto-occipital articulation (1), it seems unlikely that more than a moderate moment about the joint can be induced passively by gravity acting on the mass of the head. It is probable that the shorter muscles articulating the atlanto-occipital joint play an important role in supporting the head and neck position during collected work. This conjecture would need to be assessed with further studies of muscular activity.

Interestingly, the line of tension created by the caudal funicular and cranial lamellar band of the NL appears to intersect the calculated centre of mass of the combined head and neck segment. If proven, this would indicate a mechanically advantageous arrangement. The NL could passively

support the combined mass of the head and neck segments against gravity, while allowing autonomous movement of the head itself for maintaining visual sight lines, vestibular orientation and feeding.

## Material Properties of the Equine Nuchal Ligament

Although both elastin and collagen are known to have visco-elastic properties under dynamic loading conditions, the strain rate induced by head/neck oscillation during locomotion is relatively slow. This suggests that the hysteresis may be dominated by collagen fibre reorientation and perhaps collagen creep within the nuchal ligament composite rather than the dynamic properties of elastin, which are seen at higher vibration frequencies (7). The difference between the maximal extension rate used during this experiment and that estimated from the kinematic data is small, and probably not very important. Since the primary difference between a canter and a gallop is in stride length rather than stride frequency, the rate of head/neck oscillation would be expected to change minimally.

The stress/strain behaviour of nuchal ligament (Fig. 3) implies that at lower strain, the properties are dominated by the elastic fibre component of the NL, with a modulus of elasticity similar to isolated elastin fibres:  $6 \times 10^5 \text{ Nm}^{-2}$  (10). In contrast, the stiffness at high strain levels is dominated by the collagen component, as the modulus approaches that seen in tendon:  $2 \times 10^7$  to  $1.4 \times 10^8 \text{ Nm}^{-2}$  (5). It is improbable that normal physiological activity results in strains at the extreme end of the measured range. However, the high stiffness may function as a safety device, protecting the other structures of the neck from becoming overstrained.

These studies have shown that the lamellar portion of the NL is an integral component of this structure's function. In particular, the most cranial lamellar band appears to carry the majority of the tensile load from the caudal funicular portion of the ligament. Therefore, the line of function

is from the withers to C2, not from the withers to the skull. This organization allows the NL to store an appreciable amount of elastic strain energy that is returned to accelerate the head and neck during locomotion.

### Acknowledgments

The authors would like to thank Pat Burke and Cornell Veterinary Pathology's Necropsy Service, Dr. J. Hermanson, Dr. K. Haussler, Kristin Polizzotto, David Lee and Paul D'Antonio for technical assistance, Dr. John Gosline for helpful advice, and Michael A. Simmons for illustrations (mas44@cornell.edu).

### References

1. Buchner HHF, Savelberg HHCM, Schamhardt HC, Barneveld A. Inertial properties of Dutch Warmblood horses. *J Biomech* 1997; 30: 653-8.
2. Clayton HM, Townsend HGG. Kinematics of the cervical spine of the adult horse. *Equine vet J* 1989; 21: 189-92.
3. Dimery NJ, Alexander RMcN, Deyst KA. Mechanics of the ligamentum nuchae of some artiodactyls. *J Zool Lond* 1985; (A), 206: 341-51.
4. Dyce KM, Sack WO, Wensing CJ. *Textbook of Veterinary Anatomy*. Philadelphia: WB Saunders 1996.
5. Elliott DH. Structure and function of mammalian tendon. *Biol Rev* 1965; 40: 392-401.
6. Gellman KS, Bertram JEA. The Equine Nuchal Ligament 2: Passive dynamic energy exchange in locomotion. *Vet Comp Orthop Traumatol* 2002; 15: 9-16.
7. Gosline JM, French CJ. The dynamic mechanical properties of elastin. *Biopolymers* 1979; 18: 2091-103.
8. Minns R, Soden PD, Jackson DS. The role of the fibrous components and ground substance in the mechanical properties of biological tissues: a preliminary investigation. *J Biomech* 1973; 6: 153-95.
9. Morocutti M, Raspanti M, Ottani V, Govani P, Ruggeri A. Ultrastructure of the bovine nuchal ligament. *J Anat* 1991; 178: 145-54.
10. Wainwright SA, Biggs WD, Curry JD, Gosline JM. *Mechanical Design in Organisms*. Princeton, NJ: Princeton University Press 1982.

### Correspondence to:

Karen Gellman DVM, PhD  
Department of Biomedical Sciences  
Cornell College of Veterinary Medicine  
Cornell University, Ithaca, New York 14853, USA  
Phone: 1 607 272 8021  
Fax: 1 607 253 3541  
E-mail: ksg1@cornell.edu